Vascular Injury of the Spinal Cord

Jasmina Boban and Majda M. Thurnher

Contents

J. Boban (✉)
Department of Radiology, Faculty of Medicine Novi Sad, University of Novi Sad, Novi Sad, Serbia

M. M. Thurnher
Department for Biomedical Imaging and Image-guided Therapy, Medical University of Vienna, Vienna, Austria

Abstract

Vascular disorders of the spinal cord are rare entities that are often underdiagnosed. It is important for a radiologist in emergency set-

M. Scaglione et al. (eds.), *Emergency Radiology of the Head and Spine*, Medical Radiology Diagnostic Imaging, https://doi.org/10.1007/978-3-030-91047-1_17

ting to be familiar with complex vascular supply of the spinal cord. In this chapter, clinical and radiological findings of spinal cord infarction and ischemia, spinal arteriovenous shunts, spinal hemorrhage, and fibrocartilaginous embolism will be discussed in detail. Clinical presentation, as well as prognosis of these entities, is variable, dependent on the affected vessel(s) and the extent of the disorder in the spinal cord. It varies from acute pain and neurological deficit (both motor and sensory disorders) to progressive myelopathy. Since successful treatment is highly influenced by timely and correct diagnosis, based both on clinical and imaging findings, it is essential to recognize these entities in an emergency setting.

1 Spinal Cord Infarction/Spinal Cord Ischemia

1.1 Definition of Entity and Clinical Highlights

Spinal cord infarction (SCI) respresents a relatively uncommon condition, often clinically and radiologically challeging. This condition is related to a high morbidity due to acute myelopathy. Patients present with severe neurological deficits, but often show satisfactory functional improvement. However, up to 20% of patients present with biphasic strokes, presenting with acute or transitory sensory deficits preceded by radiant pain in the region between the shoulders (Vuong et al. 2016).

Clinical presentation is highly dependent on the affected vessel and the extent of infarction. It usually presents with acute pain, weakness, and sensation loss. The development of symptoms is quick, accounting for a few minutes up to 12 h. In 59% of patients, acute radicular pain along the distribution of radiculomedullary artery occurs (Romi and Naess 2016). Clinical syndromes as commonly observed are the following:

1. Anterior spinal artery syndrome, consisting of flaccid tetra/paraplegia with a loss of pain and temperature (bilaterally), and preserved proprioception and vibration sensations.
2. Incomplete syndrome, the spinal artery syndrome (involving only anterior horns), presenting with acute paraplegia (pseudopoliomyelitic form), painful brachial diplegia ("man-in-the-barrel" syndrome), and progressive distal amyotrophy (chronic phase).
3. Posterior spinal artery syndrome presents with a loss of proprioception and vibration sensations below the level of injury, more commonly unilateral.
4. Brown-Sequard syndrome (central artery syndrome) is ipsilateral spastic paraparesis with loss of pain and temperature sensation on the contralateral side.
5. Transverse infarct presents with bilateral motor deficits and complete sensory loss.

A separate entity is spinal transient ischemic attack lasting for several minutes to a few hours, described in a variety of clinical settings, extremely unusual.

Zalewski and his group recently proposed diagnostic criteria for spinal cord infarctions and divided them into five groups: definite spontaneous, probable spontaneous, and possible spontaneous, as well as definite periprocedural and probable periprocedural (Zalewski et al. 2019). Spontaneous SCI encompasses those not directly associated to trauma or certain procedure; they are considered rare, although often underdiagnosed (recent studies reported that 14–16% of reported transverse myelitis were ultimately diagnosed as SCI) (Barreras et al. 2018; Zalewski et al. 2018). Recently proposed diagnostic criteria include three major components as follows:

1. clinical features,
2. MRI of the spinal cord.
3. cerebrospinal fluid analysis.

Typical clinical features include rapid development of severe neurological deficit (within

12 h). More prolonged onset of neurological deficit associated with spinal cord favors alternative diagnoses. However, the evolution of deficit is commonly slower than that in cerebral infarction due to more powerful arterial collateralization. Nevertheless, small cross-sectional area of the spinal cord makes the surrounding tissue more susceptible to edema and compression that contributes to clinical worsening.

1.2 Epidemiology/Demographics

Spinal cord infarction occurs rarely in comparison with cerebral strokes, accounting for 0.3–1% of all insults, 1–2% of all vascular neurologic pathologies, and for approximately 6% of all acute myelopathies (Vargas et al. 2015). Spontaneous ischemic strokes are the most common variant of spinal cord ischemia, presenting in around 86%, while hemorrhagic strokes account for around 9% of cases (Romi and Naess 2011). Patients with spinal cord stroke are younger and more commonly females, compared to cerebral strokes. Mean age at presentation is 56 years (Sullivan and Sundt 2006). Interestingly, less commonly, these strokes are associated with hypertension and concurrent cardiac disease (Jorgensen et al. 1994). However, risk factors associated with accelerated atherosclerosis (diabetes mellitus, smoking, peripheral artery disease, and elevated cholesterol levels) are commonly observed as risk factors (Ghandehari et al. 2010; Naess and Romi 2011). Younger and male patients usually present with more severe clinical findings in the initial phase. However, these patients show much better long-term functional recovery compared to females and older patients, in whom complications during hospital stay (pneumonia, thromboemolic events) are more often encountered (Naess and Romi 2011). There are not many studies on long-term mortality among these patients. Those available report incidence of about 23% in 7 years follow-up period and 9% in 4.5 years follow-up, which is lower than in cerebral stroke patients (Nedeltchev et al. 2004; Hanson et al. 2015). High long-term mortality is associated with higher age at presentation, severity of acute neurological deficits, and the extent of peripheral artery disease (Robertson et al. 2012; Hanson et al. 2015). Up to 80% of patients with spinal cord infarction report chronic pain on long-term follow-up, while symptoms commonly reported in cerebral stroke patients, such as fatigue, depression, and cognitive deficits, occur more seldom (comparable with incidence in healthy individuals) (Naess et al. 2005).

1.3 Pathophysiology

Spinal cord infarct is caused by acute restriction of spinal cord arterial blood supply (due to embolus or plaque), leading to depletion in oxygen and glucose delivery to grey and/or white matter, which results in ischemia and infarction. This further causes acute spinal cord-related neurological deficits that are almost always clearly associated with the vascular territory of the affected artery. Perfusion restriction can occur as a result of either global flow insufficiency or occlusion of selective radiculomedullary artery. Venous origin of the infarct is present in the cases of arteriovenous fistula, leading to increased venous pressure and vasogenic edema. If prolonged, it leads to the deprivation of arterial perfusion and cytotoxic edema. Additionally, it can be found in coagulopathies, epidural infections (epidural venous thrombosis), and myelopathy caused by cervical spinal stenosis ("snake-eye" sign).

The mechanism and exact pathogenesis of this disorder remain undetermined due to lack of large populational studies that would include associated vascular diseases and comorbidities that involve vertebral bodies (Kumral et al.). Etiological factors are various and several risk factors have been identified over time: hypertension, smoking, hyperlipidemia, diabetes mellitus, as well as coronary artery disease, peripheral vascular disease, and atrial fibrillation. Mechanisms of infarction reported in the literature also vary, with majority of patients presenting with idiopathic SCI due to atherosclerotic risk factors,

followed by fibrocartilaganeous embolism, aortic dissection, hypercoaguability, vertebral artery dissection, systemic hypotension (in shock), cardioembolism, and vasculitis. Iatrogenic factors have to be taken into account, including vascular surgery (aortic cross-clamping, aortic stent-grafting, lumbar sympathectomy, splenectomy, nephrectomy, and others) and anesthetic procedures (epidural anesthesia, intercostal, and coeliac plexus block).

For the interpretation of spinal cord infarctions, it is necessary to be aware of complex vascular supply of the spinal cord. The first region of the spinal cord vascularization is located between craniocervical junction and T3 level. Cervical part of the spinal cord is supplied from one or two segmental radiculomedullary arteries, typically at the level of C3, and accessory artery at C6 and/or C8. These arteries most commonly branch off vertebral arteries, but there are some alternative pathways (the occipital artery, the ascending pharyngeal artery, the deep cervical artery, or the ascending cervical artery). The second region of vascularization extends from T3 to T7 and is supplied from the intercostal arteries. In about 70% of patients, in the upper thoracic region, an additional dominant radiculomedullary artery, called artery of von Haller, can be present. The third region extends from T8 up to the conus medullaris and is supplied by the Adamkiewicz artery (branch of intercostal artery, at the level between T9–12).

Intrinsic arterial circulation of the spinal cord is divided into the central and peripheral system. The central system supplies the gray matter and central parts of the spinal cord and is provided by the penetrating branches of central arteries (branches of the anterior spinal artery). The peripheral system vascularizes primarily white matter via radicular arteries (that are up to 5 times smaller in diameter compared to the central arteries), branches of the posterior spinal arteries. The contribution of anterior spinal arteries is much larger, and comprises about two thirds to four fifths of the transverse cross-sectional area of the spinal cord. What is also interesting is that neither transverse nor rostrocaudal anastomoses between central and peripheral systems are hemodynamically significant, except in the superficial part of conus medullaris (cruciate anastomosis or conus arcade).

Venous system of the spinal cord drains the instrinsic parts in a symmetrical centrifugal manner. Deep central regions are drained symmetrically through anterior median spinal vein and the posterior median spinal vein, while superficial regions (white matter mostly) are drained by radial veins into coronal venous plexus on the pial surface. There are rich anastomoses between these two systems. Deep veins (the anterior and posterior median spinal veins) drain through ventral and dorsal radiculomedullary veins into segmental spinal veins. Radiculomedullary veins are present on several segments only (5–10 both dorsally and ventrally). The extradural intervertebral veins communicate directly with the spinal epidural venous plexus, Batson's plexus. The intervertebral veins drain into the ascending lumbar or azygos venous systems.

At each level of the spinal cord, there is one anterior and two posterior spinal arteries. Additionally, at many levels, there are radicular arteries that run along nerve roots and supply anterior spinal arteries. The anterior spinal artery gives rise to the central arteries that supply the anterior horns and anterior parts of lateral columns of both sides. The pial plexus surrounds the spinal cord.

1.4 Imaging Technique and Recommended Protocol

The radiologist plays an important part of diagnostic cascade in these conditions, which can mimic non-vascular pathology both clinically and radiologically. Non-contrast computed tomography (CT) and spinal CT angiography (CTA) are generally not very helpful in the imaging of spinal cord infarction. However, in older patients, detection of atherosclerosis or vascular lesions after surgery can indirectly aid to the diagnosis.

MRI is the imaging modality of choice for the diagnosis of the spinal cord ischemia and differential diagnoses, revealing acute lesions in up to

70% of patients with suspected diagnosis (Harringan and Deveikis 2013). The proposed protocol should include the following:

1. T1-weighted sagittal spin-echo.
2. T2-weighted sagittal spin-echo,
3. short-tau inversion recovery (STIR) sagittal,
4. T2-weighted gradient-echo axial sequences.

Diffusion-weighted imaging (DWI) is not routinely performed in majority of the centers, but aids to the diagnosis. DWI can be acquired in sagittal or axial plane. Sagittal plane has the advantage of a larger coverage in shorter time, while axial acquisition allows visualization of restricted diffusion on both sides of the spinal cord and is useful in differentiation of this entity from similar conditions.

Contrast study aids to the diagnosis since enhancement is usually absent in the acute stage. T1-weighted postcontrast study contributes to the differential diagnosis in indefinite cases. Additional diagnostic studies might include magnetic resonance angiography, CTA, and digital subtraction angiography (especially in cases of suspected thrombus in the abdominal aorta, or Adamkiewicz artery).

MRI findings that are required for diagnosis of SCI are as follows:

1. no findings of spinal cord compression,
2. specific finding of DWI restriction, associated vertebral body infarction, or arterial occlusion/dissection adjacent to the lesion,
3. supportive: intramedullary T2-hyperintense lesions (Zalewski et al. 2019).

It is important to support the diagnosis with analysis of cerebrospinal fluid, primarily in order to exclude inflammatory etiology (cell count, IgG index, oligoclonal bands).

1.5 MRI Findings

Findings on MRI can be normal in up to one fourth of patients. Usually, the most informative findings are identified on T2W sequence, with hyperintensity in the central cord more than in the peripheral, and usually in longer than one vertebral section. A common finding is associated T2W/STIR hyperintensity in the vertebral bodies (medullary bone) due to vertebral body infarct (Fig. 1). There are six different spinal stroke syndromes identified on MR imaging.

The anterior spinal artery infarction represents the most common SCI syndrome and is limited to the anterior horns and the surrounding white matter (classic “owl’s eyes” or “snake eyes” sign, Fig. 2). The anterior unilateral infarct unilateraly affects anterior horn. Posterior spinal artery infarct is limited to the posterior columns, but may extend to the posterior parts of lateral columns. Posterior unilateral infarct is restricted to one posterior horn and sometimes extends into the posterior part of ipsilateral lateral column/posterolateral region. Central infarct is located around the anterior sulcus, in the shape of crescent. Transverse infarct involves anterior and posterior columns and extends to both anteo- and posterolateral regions.

Diffusion restriction is present, following the similar pattern as in the cerebral stroke. Restriction is demonstrated approximately hours after the onset of symptoms, with pseudo-normalization after approximately 1 week (Peckham and Hutchins 2019). Typical contrast enhancement in SCI is linear craniocaudal strip of enhancement, reflecting the predominant ischemic area, usually in the grey matter and confirmed to a specific arterial territory. During the subacute phase, the patchy contrast enhancement is observed, usually after 5 days and lasting for approximately 3 weeks. In general, contrast enhancement is suggestive of alternative diagnoses, at first transverse myelitis. However, in up to one half of periprocedural SCIs and in around 40% of spontaneous SCIs contrast enhancement is observed.

If the SCI is not confirmed after initial imaging and the clinical suspicion remains the same, a follow-up imaging is recommended (days later).

Fig. 1 Conus medullaris infarction followed by infarction of the vertebral body. Conus medullaris is enlarged and swollen (**a** – T2W sagittal image), with no contrast enhancement (**b** – T1W FS postcontrast image). Clearly defined geographic area of the lack of contrast enhancement is observed in the posterior part of L1 vertebral body (**c** T1W FS sagittal image), corresponding with vertebral body infarction. On cross-sectional area of the spinal cord, "owl-s eyes" sign is evident on T2W axial image (**d**), followed by diffusion restriction (**e**), reflecting anterior spinal artery infarction

1.6 Differential Diagnosis and Pitfalls

The differential diagnosis of the spinal cord infarction is actually wide, given this is a rather rare entity. The main differentials include multiple sclerosis (MS), neoplastic lesions, idiopathic transverse myelitis, and venous congestive myelopathy.

Multiple sclerosis lesions are usually located in the peripheral white matter and comprise not more than three segments in craniocaudal direction and not more than a half of cross-sectional area. Additionally, they are commonly associated with brain lesions and have a different and relatively distinct clinical presentation.

Spinal cord neoplastic lesions present with characteristic expansion of the cord associated with nodular or diffuse enhancement after contrast. Also, cystic degeneration is common. Clinical onset is slow.

Idiopathic transverse myelitis can have similar clinical presentation, but not as acute (SCI occurs in several minutes!). The lesion is long (usually over three segments) and occupies more than two thirds of cross-sectional area.

Fig. 2 Anterior spinal artery infarction. A "pencil-like" T1 hypointense (**a**), T2-hyperintense (**b**) lesion is observed in the anterior aspect of the spinal cord on T4–7 level, with corresponding "owl's eyes" sign on the axial image (**c**), reflecting typical artery of Adamkiewitz infarction, after stent graft repair of thoracic aorta (**e**) due to dissection (**d**)

Venous congestive myelopathy is characterized by the presence of engorged pial veins associated with T2W/STIR-hyperintense signal in the central and peripheral white matter.

2 Spinal Arteriovenous Shunts

2.1 Definition of Entity and Clinical Highlights

Spinal arteriovenous (AV) shunts are rare lesions.

Numerous classification systems exist for these lesions, based on different features of the lesions (Da Costa et al. 2009). The Anson-Spetzler classificiation is based on the flow pattern and angio-architecture and therefore compatible with the imaging patterns.

1. Type I: dural AV fistula (dAVF) represents the most common type of shunt lesion, accounting for 60–80% of these lesions. This is a low flow lesion found typically in lower thoracic or lumbar spine, with a rather small probability to produce hemorrhage or to generate aneurysmatic dilatation of the vessel wall (Rodesch et al. 2004).
2. Type II: intramedullary glomus AV malformations (glomus type), representing an intradural spinal AV shunt lesion, accounting for 10–15% of the lesions. Sometimes they are referred to as pial AVMs. These high flow lesions occur throughout spinal cord and are characterized with plexiform nidus of multiple AV shunts, with feeding arteries often raising from the anterior or posterior spinal arteries and draining veins going to perimedullary veins. The incidence of associated anurysms is up to 10%.
3. Type III: Juvenile AVMs (spinal AV metameric syndrome, Cobb's syndrome) are extremely rare (up to 5% of all spinal AV shunt lesions). This is a developmental syndrome, representing a combined high flow intramedullary and extramedullary lesion due to dysfunction of vasculogenic embryionic tissues. They are usually located in cervical and upper thoracic spine and can be associated with both arterial and venous aneurysms (Gros & Du, 2014).
4. Type IV: intradural perimedullary AV fistula, accounting for 15–25% of all spinal AV shunts. These lesions are high flow but low pressure lesions, located anteriorly in the region of conus, fed by the anterior spinal artery. Arterial aneurysms and venous ectasias are common.

Clinical presentation is variable and can point to the specific type of the lesion. dAVFs usually present with radicular or non-radicular pain and slowly progressive neurological deficits (over months). Glomus type lesions present usually with acute spinal cord hemorrhage followed by severe pain described as "dagger stab". Progression of myelopathy occurs secondary to repeated hemorrhages (due to aneurysms or subarachnoid hemorrhage from the nidus). However, this is in general a condition with good prognosis and up to 80% of patients are independent in 5 year period. Type III lesions (metameric syndrome lesions) occur in children and young patients, presenting with progressive myelopathy and associated with poor prognosis. Intradural perimedullary AVFs present with progressive neurologic deficits due to venous congestion. Sometimes, subarachnoid hemorrhages occur in up to 1/5 of patients. The outcome is poor, with a complete loss of spinal cord function in 10–20 years after the onset (Fugate et al, 2021, Rosenblum et al. 1987).

2.2 Epidemiology/Demographics

dAVF has a strong male predominance, occurring mostly in middle aged men (40–70 years of age). Glomus type AV shunts are typically found in younger patients below the age of 40 (50% patients are younger than 25), with no sex predilection. However, up to ¼ is associated with neurocutaneous syndromes (hereditary hemorrhagic teleangiectasia—Osler-Weber-Rendu). Intradural perimedullary AV fistulae occur most frequently in younger patients, age 20–50, with no sex predilection. Like glomus type, type IV lesions

present a rather strong association with neurocutaneous syndromes.

2.3 Pathophysiology

Symptoms of dAVFs present secondary to the medullary venous hypertension and congestion. These conditions are worsened by bending coughing, exercise, and pregnancy.

2.4 Imaging Technique and Recommended Protocol

Non-contrast CT is generally not used for the initial diagnosis, nor for the follow-up. The most common imaging modality used is contrast-enhanced MRI, usually followed by an angiographic examination, such as CTA or DSA.

The recommended protocol includes the following:

1. T1-weighted sagittal spin-echo.
2. T2-weighted sagittal spin-echo,
3. short-tau inversion recovery (STIR) sagittal,
4. T2-weighted gradient-echo axial sequences.
5. T1-weighted contrast-enhanced sagittal and axial tomograms.

Steady state sequences (CISS, FIESTA) are extremely useful due to heavy T2 contrast that increases sensitivity in detection of flow voids.

Susceptibility weighted imaging is a promising toll in the evaluation of hemosiderin deposits in the spinal cord, but has not yet fully entered clinical practice. However, there are some reports on the signs that can be observed in cases of chronic myleopathy caused by dAVFs (Enokizono et al. 2017).

2.5 MR Imaging

dAVFs have a typical presentation on MRI with prominent perimedullary vascular flow voids (especially on steady state sequences). Spinal cord is usually expanded due to edema (venous congestion and hypertension) with T2 hyperintensity in the central parts and sparing of the most peripheral parts (Fig. 3). Peripheral parts of the cord sometimes show T2 hypointensity, suggesting susceptibility changes in relation to venous deoxygenation. Small pial vessels often show enhancement, but this sign sometimes can also be absent (Krings et al, 2005). Enokizono et al. demonstrated the presence of "black butterfly sign" in the dorsal aspect of medulla and the central grey matter, probably representing hemorrhage, best observed on T2* and SWI images, although detectable on T2W also. The presumed mechanism of this finding was the prolonged venous congestion (Enokizono et al. 2017). CTA shows ectatic perimedullary veins, dilated transdural draining vein, and plexiform nidus at the level of neural foramen. DSA remains the gold standard for fistula localization and is used as a diganostic modality of choice for preoperative planning. DSA presents the pathognomonic finding of retrograde flow in transdural vein with dilated transdural radicular vein that fills tortuous perimedullary veins retrogradely (Fig. 4).

Glomus type fistulas show intramedullary nidus with expanded cord due to parenchymal edema and intramedullary blood products. Feeding vessels are usually derived from the anterior and posterior circulations, while the drainage is to large perimedullary veins (Krings et al. 2007). They are usually found in the thoracolumbar spine. Sometimes they can have associated aneurysms and consequent subarachnoid hemorrhage. DSA is essential for diagnosis of these lesions, with clear delineation of the nidus itself, feeding vessels, and draining veins. MRI is not a reliable imaging modality in preoperative planning (Rubin and Rabinstein 2013).

Type III fistulas present with tortous and ectatic vessels within the spinal cord, associated with subarachnoid and epidural spaces arranged in metameric distribution. Numerous high flow AV shunts are observed on DSA, and AVMs and spinal cord share the same blood supply. Bone, muscle, and skin are often involved in the abnormality.

Type IV fistulas show anterior perimedullary flow voids, often with displacement of the spinal

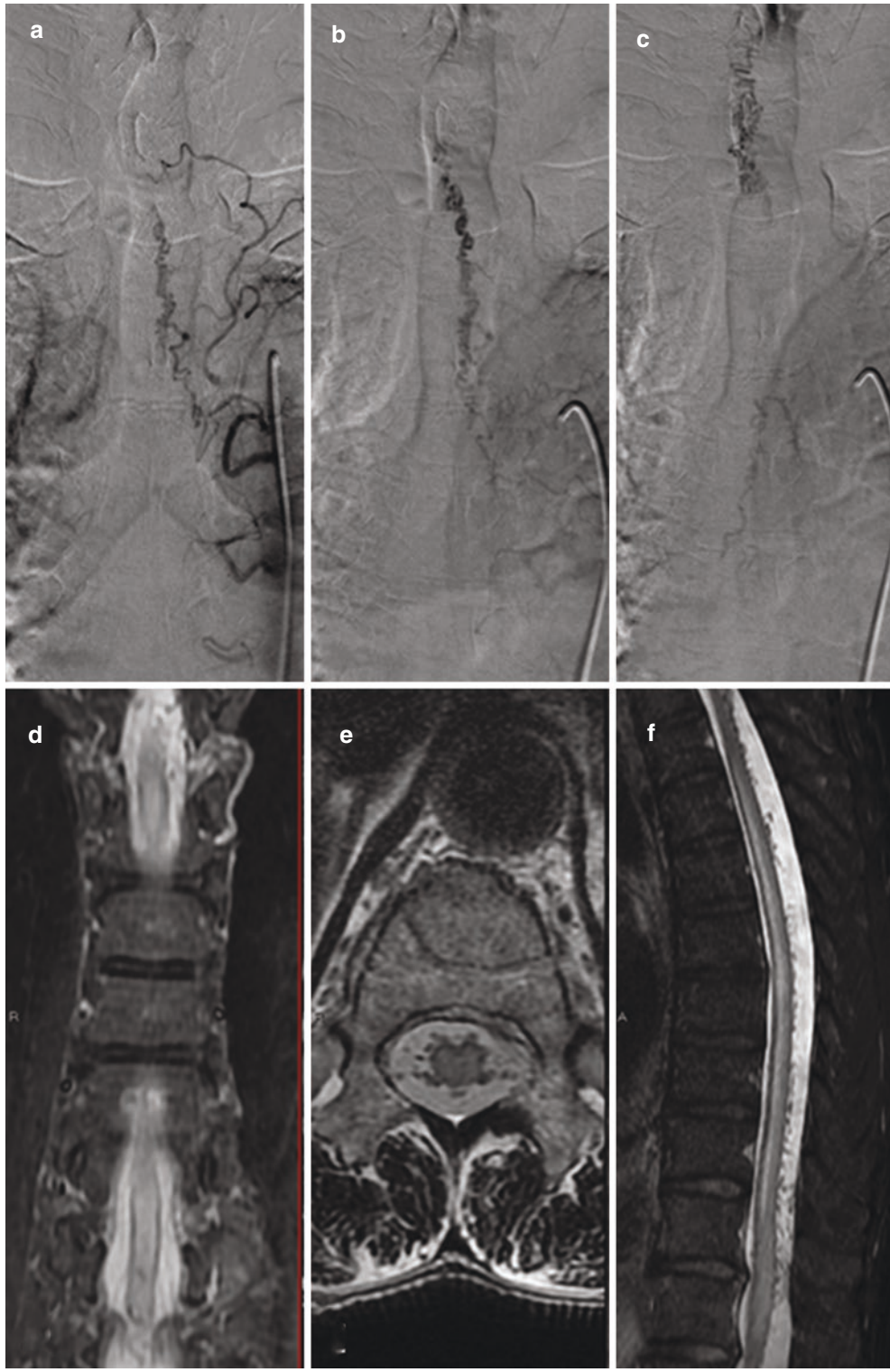

Fig. 3 Spinal dural arteriovenous fistula. The thoracic part of the spinal cord is swollen (**a**, T2W coronal image), due to spinal dural AVF at the level of T5, with evident tortous dilated perimedullary veins around the whole circumference of the spinal cord on the cross-sectional area (**e**, axial image), although most conspicuous on the posterior surface (**f**, STIR sagittal image). DSA shows slow filling of the dilated perimedullary veins (**a**–**c**)

Fig. 4 Spinal dural arteriovenous fistula. Spinal cord is enlarged and swollen in the lower thoracic part (**a** – T2W sagittal image), with evident tortous and dilated perimedullary veins on the posterior surface (**b** – postcontrast T1W FS sagittal image), representing dural arteriovenous fistula. In the lower part of thoracic medulla, one can observe "The missing piece" sign, focal geographic area with the lack of contrast enhancement within a long segment of intense holocord contrast enhancement (Zalewski et al. 2018)

cord posteriorly due to ectatic subarachnoid varices. Often, there are signs of medullary edema and expansion. DSA might show a superficial extra-axially localized nidus with arterialized perimedullary vein.

2.6 Differential Diagnosis and Pitfalls

The key problem in the MRI of the AV shunt lesions is the fact that often only abnormality within the spinal cord is observed, limited to the abnormally high T2 signal and expansion of the cord due to edema. The main differential diagnosis in this case is venous congestive myelopathy. Other differential diagnoses include infarction, demyelination, infection, and neoplasms.

Heavily weighted T2 sequences are helpful in accentuating enlarged and tortuous vascular structures on the dorsal or ventral surface of the cord, which are suggestive of diagnosis. Additional aid can be obtained by T1 contrast-enhanced tomograms that enable visualization of the abnormal leptomeningeal vessels. However, prominent perimedullary vessels are not specific for AV shunts. The same finding can be observed in some tumors, such as hemangioblastomas, or hypervascular schwanommas.

3 Spinal Hemorrhage

3.1 Definition of Entity and Clinical Highlights

Spinal hemorrhage is a rare but important clinical entity, classified according to the anatomical space that is involved in the pathological process. Most of the cases are due to trauma, second most common forms (up to 35%) are idiopathic; most common nontraumatic causes are coagulopathies and vascular malformations (Novy et al. 2006; Baaj 2012).

Spinal hemorrhage manifests with acute, painful myelopathy, neck or back pain. Signs and symptoms usually reflect the level of injury, the extension of the bleeding, and the acuity (Shaban et al. 2018). Symptoms may also develop subacutely (in weeks). It is important to know that slowly progressive course is very rare, seen in less than 5% of patients (Kreppel et al. 2003). SAH in the spine presents similarly like intracranial SAH, with acute headache, meningismus, or other meningeal signs (Swann et al. 1984). In addition, in spinal SAH, cranial symptoms such as headache, seizure, altered mental state, and nausea can be found (Kreppel et al. 2003). Smaller hematomas may be managed conservatively. However, since neurologic deficits can be reversible, surgical decompression is often considered (Pierce et al. 2018).

Neck or back pain is usually the leading symptom, observed at the level of hemorrhage, sometimes radiating to extremities. The hallmark of SAH is so-called “le coup de pignard” or “dagger’s stab”. Progressive neurological symptoms including sensory loss, bowel or bladder disturbances are usually result of venous congestion in progressive forms of myelopathies.

3.2 Epidemiology/Demographics

Spinal epidural hematoma (EDH) occurs in approximately 0.1/10,000 people annually and represents the most common form of spinal hemorrhage. Meta-analysis showed that 75% of all spinal hematomas are epidural (Kreppel et al. 2003). SAH in the spine is the second most common form of spinal hemorrhage. Nevertheless, this condition is extremely rare and occurs in approximately 6/100,000 people annually. Spinal subdural hematoma (SDH) and intramedullary hematoma (IMH) are two least common forms of spinal hemorrhage. SDH occurs in about 4% of cases with spinal hematomas. Hematomas occupying multiple compartments account for 2.1% of all spinal hematomas (Moriarty et al. 2019). The etiology of spinal cord hemorrhage is listed in Table 1.

Table 1 Etiology of spinal cord hemorrhage

Epidural hemorrhage/ hematoma	Iatrogenic (spinal procedure, antiplatelet, anticoagulant therapy) Trauma Vascular diatheses
Subdural hemorrhage/ hematoma	Iatrogenic Trauma Coagulopathy
Subarachnoid hemorrhage	AVM Spinal aneurysm, AVF Trauma Iatrogenic Rare: metastases, vasculitis, hemangioblastoma, ependymoma
Hematomyelia	Trauma AVM, cavernoma, AVF Anticoagulant therapy Bleeding diatheses Primary or secondary tumors Rarely: aneurysms, irradiation

3.3 Pathophysiology

EDHs represent the most common form of spinal hmorrhage (Kreppel et al. 2003). Most frequently, they are caused by epidural venous plexus hemorrhage due to minor trauma, coagulopathy, or disc extrusion. Sponatenous EDH has an incidence of 0.1/100,000 person-year. SDH is caused by iatrogenic factors in up to 70% of cases; less commonly, it is caused by trauma, surgical procedure, coagulopathy, neoplasm, or AVMs. The pathogenesis is associated with collapse of the microvasculature between dura and arachnoidea due to minor trauma. Approximately 1% of all SAHs are caused by primary spinal cord pathology, usually spinal AVMs, dAVFs, spinal aneurysms, and hemorrhagic tumors (Shaban et al. 2018). Commonly, SAH in the spine occurs as a secondary phenomenon, associated with intracranial aneurysm rupture. Spinal SAH also can happen as a result of spinal artery aneurysms (type I aneurysms are related to lesions that increase arterial blood flow, while type II are isolated forms). Spinal aneurysms have predilection for the anterior spinal artery and cervical spine (50%). They are usually fusiform, without the neck, and result from intimal dissection (Vuong et al. 2016). IMH or hematomyelia are described rarely, most commonly related to anticoagulant treatment, or trauma, neoplasms (Novy et al. 2006; Agarwal et al. 2014). Trauma represents the most common cause of hematomyelia, usually seen in the cervical cord (Pillai et al. 2008). The source of bleeding is microcirculation, creating mass effect that later results in local infarction caused by hypoxia and ischemia (Dumont et al. 2001). Vascular malformations associated with hematomyelia are AVMs and cavernomas; however, AVM usually leads to spinal SAH (Allen et al. 1979). AVFs can also sometimes cause hematomyelia, usually associated with hemorrhagic transformation of venous infarction (Mascalchi et al. 1998). Old-fashioned anticoagulant therapy has been associated with hematomyelia; however, there are no cases reported with new anticoagulants.

3.4 Imaging Technique and Recommended Protocol

MRI with contrast injection is the preferred diagnostic modality in evaluation of spinal cord hemorrhage. The recommended protocol consists of T1W, T2W, gradient-echo imaging or SWI, and DWI. Additional imaging usually refers to dedicated imaging of the vessel pathology, such as MRA, CTA, or DSA. DSA remains the gold standard for identification of vascular pathology (Shaban et al. 2018). Location of the hemorrhage source remains extremely challenging, even with spinal angiography, especially in the cases of isolated aneurysms.

Evaluation of the spinal hemorrhage requires the understanding of blood products' presentation on MRI, which is time-dependent. The principles of five stages of hemorrhage, described already for decades on MRI of the intracranial hemorrhage, can be applied to spinal hemorrhage as well (Table 2).

It is important to identify the precise localization of hemorrhage before the surgical exploration. The position of hematoma in relation to dura is the key feature for differentiation between subdural and epidural hematomas. This position can be best identified on MRI, using both axial and

Table 2 Evolution of the hemmorhage on MRI

Stage	Time period	Blood component	T1W	T2W	T2W*/SWI
Hyperacute	<24 h	Oxyhemoglobin	Hypo	Hyper	Variable/Negative
Acute	1–3 days	Deoxyhemoglobin	Iso	Hypo	Hypo rim
Early subacute	3–7 days	Intracellular methemoglobin	Hyper	Hypo	Hypo
Late subacute	1–2 weeks	Extracellular methemoglobin	Hyper	Hyper	Hypo
Chronic	>2 weeks	Hemosiderin	Hypo	Hypo	Hypo

sagittal imaged, by identifiying the fat, which is basically never affected by SDH (Kobayashi et al. 2017). Classic star-like appearance of filum terminale and cauda equina roots that are affected by SDH is called the inverted Mercedes-Benz sing (Hausmann et al. 2001).

MRI features of the spinal hemorrhage evolve with time (Table 2). On CT and MRI, spinal artery aneurysm presents as a focal fusiform dilatation of an intradural spinal vessel (usually radiculomedullary artery). They are usually very small.

EDH can be recognized in the posterior, anterior part or diffuse around the dural sac, with a specific loss of epidural fat signal and smooth contour towards the spinal canal (Figure). Seventy-five percent of the cases present with EDH dorsally or dorsolaterally within the spinal canal. This is the result of dura being more tightly attached to the posterior longitudinal ligament than yellow ligaments.

SDH occurs in the potential space between dura and arachnoidea and can be identified as separated from the epidural fat with prominent black line that represents dura. It is always contained within the wall of thecal sac. Key feature in differential diagnosis from EDH is the presence of epidural fat without inward displacement of the hypointense dura mater (Moriarty et al. 2019). The inner contour of SDH is concave but usually irregular, not smooth like in EDH. SDH generates mass effect on the cord, which is one of the important characteristics of this hematoma in differential diagnosis (Mashiko et al. 2006). Blood in the thecal sac compresses nerve roots and cord and produces the inverted Mercedes-Benz sign. Contrary to EDH, SDH does not extend into neural foramina and also does not make direct contact with the bone.

SAH usually extends in a longitudinal direction, as layering blood in the CSF space, without producing a focalized abnormality (Flanders et al. 1999). Sometimes, it can present as non-enhancing intradural extramedullary clot with mass effect on the spinal cord and nerve roots (Pierce et al. 2018). Distinguishing feature of SAH is the presence of sedimentation and fluid-fluid levels typically observed in the dependent lower lumbar region, and also the presence of epidural fat signal. Mass-like blood clot is observed rarely, with variable signal intensity on T1W and T2W images, but always with CSF signal intensity surrounding the hematoma, and thus allowing differentiation from other types of spinal hematomas.

Intramedullary hemorrhage (hematomyelia) represents blood products within the spinal cord parenchyma or syrinx (Fig. 5). It usually occurs at the point of maximal impact in trauma, most often confined to the central grey matter in the form of hemorrhagic necrosis (Looby and Flander 2011). T2* or SWI images are recommended for the proper delineation of blood products. Often, associated finding is rather extensive medullary edema, extending both cranially and caudally from the hemorrhagic lesion (Moriarty et al. 2019). Spinal hemorrhage can affect multiple compartments, thus causing diagnostic challenge. In these cases, systematic analysis of each compartment is essential for understanding the extent of the disorder.

3.5 Differential Diagnosis and Pitfalls

Careful evaluation of the signs for each compartmental hemorrhage is necessary, especially in cases of multicompartmental hemorrhage.

Fig. 5 Hematomyelia. In the lower thoracic part of the spinal cord, heterogenous signal intensity can be observed, with T2 hypointense (**a**) and T1-hyperintense (**b**) areas, corresponding to SWI hypointensities (**c**), representing areas of subacute hemorrhage

Differentiating spinal hematoma from inflammation and neoplasm can be challenging. Neoplastic process shows contrast enhancement, at least marginal. Marginal enhancement can seldom be observed in the hyperacute phase of spinal hematoma (Chang et al. 2003). However, clinical history is different. Clinical history is also an important key to the diagnosis in inflammatory process, such as abscess or spondylodiscitis.

EDH should be distinguished from epidural tumor spread or metastasis (breast, lung, and prostate cancer). Epidural tumor is usually T1 hypointense, with more solid contrast enhancement. Identification of concomitant vertebral body infiltrative lesions helps in establishing the right diagnosis. Epidural abscess is an epidurally located fluid collection with heterogenous signal intensity, but shows the same mass effect as EDH. However, it typically occurs with discitis/osteomyelitis, as well as with destruction of the bone or paraspinal muscle fluid collections and inflammatory reaction. Rarely, differential diagnosis includes epidural disc sequestra, fibrosis due to postsurgical state, and facet synovial cysts (Pierce et al. 2018).

Differential diagnosis of SDH includes subdural abscess and hygroma, generally aided by clinical findings and history. Spinal subdural abscess is an extremely rare entity, presenting with fever and back pain. On the imaging, it has a complex signal intensity with peripheral enhancement, with no abnormalities on gradient-echo imaging. Subdural hygroma is observed in patients with recent trauma or intervention. They usually present with signal intensity similar to CSF space. Intradural extramedullary masses (meningeomas and nerve sheath tumors) typically enhance avidly and homogenously. Arachnoiditis can also be included in differential diagnosis, resulting in the grouping of cauda equina nerve roots.

It is important to differentiate the presence of subarachnoid spinal hematoma from the flow voids of cerebrospinal fluid (CSF). CSF does not generate mass effect and compression on the cord, as SDH. In addition, spinal hematoma is identifiable on all MR sequences, while CSF flow voids are usually most prominent on T1W/T2W sequences, but disappear on gradient-echo sequences. In addition, there is no compressive effect on the spinal cord and nerve roots. Sometimes it is hard to differentiate SDH from SAH, but the latter lacks fluid-fluid levels, which can be a helpful hint.

IMH should be differentiated from intramedullary neoplasm, especially in the cases of nontraumatic etiology (when clinical history is not helpful). In these cases, neoplasm should be considered a potential underlying cause of IMH. Both primary (hemangioblastoma and ependymoma) and secondary tumors (metastases, most commonly from renal cell, breast, and lung carcinoma) can produce hemorrhage. Ependymomas may present with peripheral rim or hypointense foci of T2 hypointensity, termed "cap sign", and enhance avidly. Hemangioblastoma is usually in the form of a cystic lesion with an intensively enhancing nodule. Metastases have variable presentation, but most commonly, they have homogenous ehncancement with great amount of surrounding edema. Spinal AVMs are also a common cause of hematomyelia, but usually have a typical MR presentation.

4 Fibrocartilaginous Embolism

4.1 Definition of Entity and Clinical Highlights

Fibrocartilaginous embolism (FCE) represents a rare condition that occurs due to migration of fibrocartilagionous nucleus pulposus through the vasculature into the spinal cord vessels (AbdelRazek et al. 2016). Up to date, no more than 200 cases nave been described in the literature (Mateen et al. 2011). However, many authors feel that this condition is actually underestimated and often overlooked cause of the spinal cord infarction (Manara et al. 2010).

Clinical picture is that of a spinal cord infarction, with the transient back or neck pain, followed by progressive myelopathy. There is always a sensory level present, with bladder and/or bowel dysfunction. Typically, paraplegia or quadriplegia (with or without respiratory compromise) occurs, dependent on the level of lesion (thoracolumbar region vs. cervical spinal cord). Symptoms occur promptly and develop over

hours, which helps in distinguishing from inflammatory or neoplastic disease. Also typically, there is temporal relationship to an event that served as a trigger for FCE (bending, minor trauma, heavy lifting) measured in hours to days. The typical clinical finding in anterior spinal infarction is the sparing of proprioception and vibration sensation below the sensory level.

The diagnosis of FCE is based on the following criteria:

1. severe acute back/neck pain followed by rapid onset of progressive paraplegia/quadriplegia with sphincter dysfunction and/or abolishment of reflexes,
2. close temporal relationship with Valsalva maneveur or a minor trauma,
3. negative CSG examination; absence of systemic embolic sources and prothrombotic conditions,
4. concordant MRI findings of a spinal cord infarction (cord edema) with signal intensity changes in the intervertebral disc or body adjacent to the level of the cord lesion or Schmorl's nodules (Spengos et al. 2006; Raghavan et al. 2004; Davis and Klug 2000).

4.2 Epidemiology/Demographics

FCE occurs slightly more commonly in females (63.5%), with the average age around 40. However, more than a half of reported cases occurred in patients younger than 40. In recent literature, the period between the trigger and FCE symptoms was average 2.4 days (usually within 24 h). Symptoms of neck or back pain were observed in more than ¾ of cases. Mortality due to this condition was most commonly associated with pulmonary embolism, pneumonia, and aspiration (AbdelRazek et al. 2006; Mateen et al. 2011).

4.3 Pathophysiology

Although intervertebral disc represents an avascular structure, it is the source of embolic material in this rare condition. Intervertebal disc consisted of two compartments: mesodermally derived annulus fibrosus and endodermally derived, centrally located nucleus pulposus. In the neonatal period, disc is supplied by rich vasculature, which regresses at the age of 2 months and the disc becomes completely avascular by the end of the first decade of life. In the normal adult, neovascularization appears at the age of 50, and in cases with developed degenerative disease, even earlier (Boos et al. 2002). Shared arterial supply between vertebral bodies and the spinal cord (spinal branches of radicular arteries supply the posterior parts of vertebral bodies and reinforce the longitudinal spinal arteries to the spinal cord) is the postulated pathophysiologic basis for the occurrence of FCE (AbdelRazek et al. 2016). Additionally, Schmorl's nodes represent *loci minoris resistentiae,* because fibrocartilaginous masses are in the close proximity to the vasculature of vertebral body. It is suggested that the initial trigger is increased intradiscal or intravertebral body pressure by axial forces during Valsalva maneuvers (heavy lifting, straining, or minor trauma to the back or neck). The fibrocartilaginous mass, after entering vasculature, travels through either arterial or venous route to reach the spinal cord. If it enters arterial route, it travels through radicular artery and causes spinal cord infarction (Yousef et al. 1998). If it, on the other hand, enters the venous route, it goes through vena cava to the Batson's plexus and spinal cord. Some cases showed the presence of both arterial and venous FCE in cases of concomitatnt arterial and venous embolizations or due to presence of normally present AV shunts in the epidural space (Vuia and Alexianu 1969).

4.4 Imaging Technique and Recommended Protocol

Imaging modality of choice is MRI, since CT is not sensitive for depiction of parenchymal lesions in the spinal cord. Recommended protocol is basically the same as for the spinal cord infarction:

1. T1-weighted sagittal spin-echo.
2. T2-weighted sagittal spin-echo,
3. short-tau inversion recovery (STIR) sagittal,
4. T2-weighted gradient-echo axial sequences.

Diffusion-weighted imaging (DWI) and contrast study are optional, but can aid to the diagnosis, especially DWI, that can also be of prognostic value.

Typical findings are that of the spinal cord infarction, with T2 hyperinetnse lesions in a vascular distribution, most commonly with no contrast enhancement (typically observed in inflammatory or neoplastic lesions). However, in the subacute phase, patchy gadolinium enhancement can be observed, as well as hemorrhagic transformation of infarction. Additional important imaging feature are T2 signal intensity changes in the vertebral body or intervertebral disc adjacent to the cord lesion (Fig. 6).

Standard, conventional MRI (without DWI) can be unremarkable, especially in the early stages. DWI might have a key role in establishing

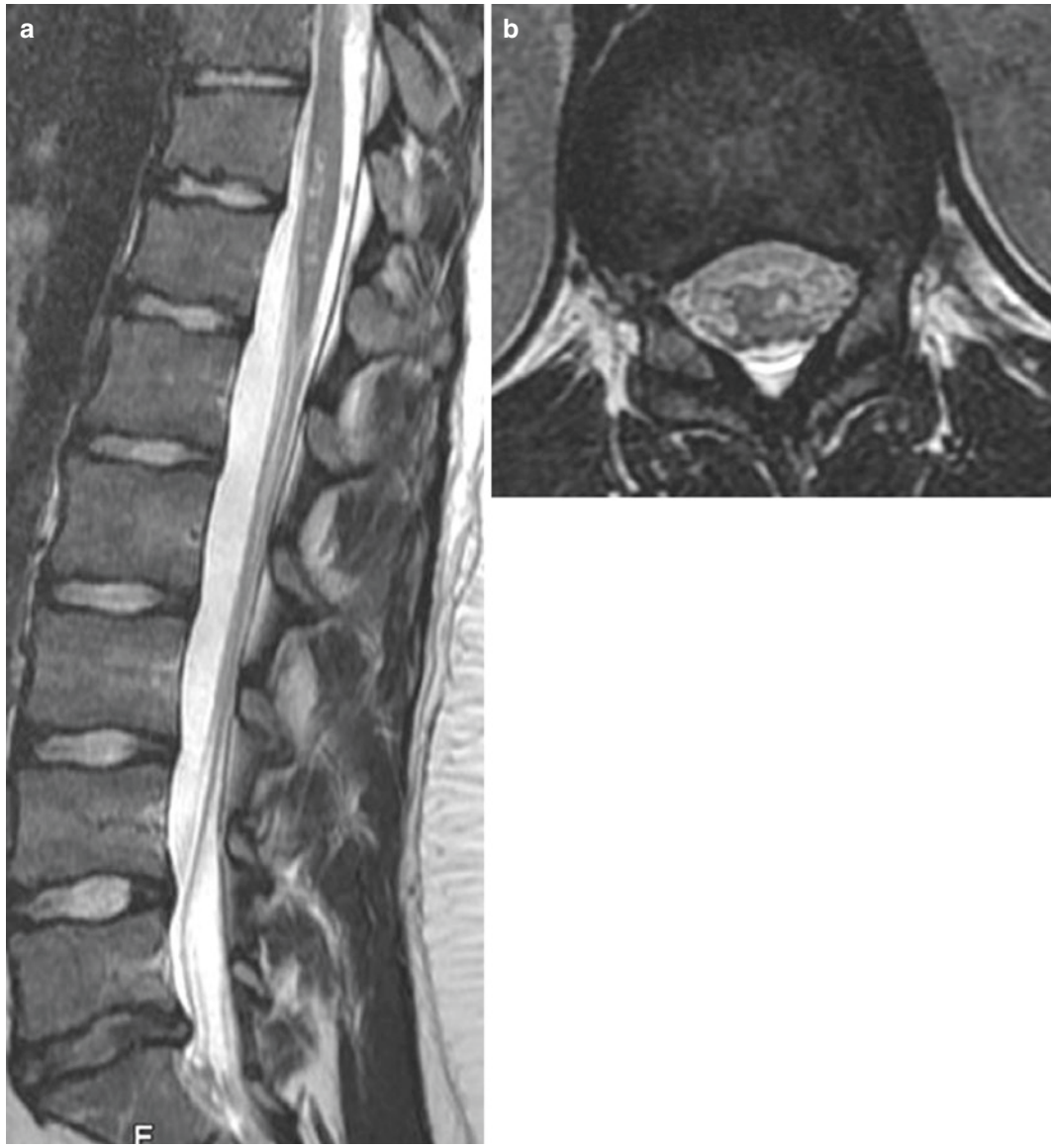

Fig. 6 Fibrocartilaginous embolism. On T2W sagittal image, lesions in the anterior part of the conus are evident (**a**), consistent with infarction of the left anterior horn (**b**). Bulging of L5-S1 intervertebral disc is observed and represents the potential source of embolism

the accurate diagnosis, since it can differentiate vasogenic (present in inflammatory myelitis) from cytotoxic edema (present in ischemia). Changes observed on DWI predate signal changes on T2 and can be observed within a few hours after the onset of ischemia (Manara et al. 2010).

4.5 Differential Diagnosis and Pitfalls

FCE remains an uncommon diagnosis and is often mistaken for the inflammatory cord lesions, based solely on imaging features. However, the likelihood of FCE raises with typical clinical presentation, the presence of a trigger in close past, along with suggestive CSF findings and MRI features of a spinal cord infarction. CSF analysis is usually normal or with slightly elevated protein level. However, pleocytosis or increased IgG levels, typical for inflammatory lesions, are never observed (Frohman and Wingerchuk 2010).

DWI is an extremely useful sequence for differentiating inflammatory myelitis from spinal cord ischemia. Ischemic lesion is first observed as diffusion-restricted area in the spinal cord in the vascular distribution, predating signal changes on T2. To the contrary, in the inflammatory lesions, signal intensity changes are well-observed on T2, while there are no concordant abnormalities on DWI (insensitive), or there can be signs of facilitated diffusion consistent with vasogenic edema. Therefore, DWI should be included in the standard protocol for evaluation of the spinal cord lesions, since it proves the ischemic nature of the lesion very early in the course of disease.

References

AbdelRazek MA, Mowla A, Farooq S, Silvestri N, Sawyer R, Wolfe G (2016) Fibrocartilaginous embolism: a comprehensive review of an under-studied cause of spinal cord infarction and proposed diagnostic criteria. J Spinal Cord Med 39(2):146–154

Agarwal A, Kanekar S, Thamburaj K, Vijay K (2014) Radiation-induced spinal cord hemorrhage (hematomyelia). Neuro Int 6(4):5553

Allen JP, McDonald JV, Horner FA (1979) Hematomyelia with arteriovenous malformation of the cord: successful surgical treatment. Arch Neurol 36:455

Baaj A (2012) Spinal emergencies. In: Handbook of spine surgery. Thieme, New York, pp 190–191

Barreras P, Fitzgerald KC, Mealy MA et al (2018) Clinical biomarkers differentiate myelitis from vascular and other causes of myelopathy. Neurology 90(1):e12–e21

Boos N, Weissbach S, Rohrbach H, Weiler C, Spratt KF, Nerlich AG (2002) Classification of age-related changes in lumbar intervertebral discs. Spine 27(23):2631–2644

Chang F, Lirng J, Chen S et al (2003) Contrast enhancement patterns of acute spinal epidural hematomas: a report of two cases. AJNR Am J Neuroradiol 24(3):366–369

Da Costa L, Dehdashti AR, terBrugge KG (2009) Spinal cord vascular shunts: spinal cord vascular malformations and dural arteriovenous fistulas. Neurosurg Focus 26(1):E26

Davis GA, Klug GL (2000) Acute-onset nontraumatic paraplegia in childhood: fibrocartilaginous embolism in acute myelitis? Childs Nerv Syst 16:551–554

Dumont RJ, Okonkwo DO, Verma S et al (2001) Acute spinal cord injury. Part I: pathophysiologic mechanisms. Clin Neuropharmacol 24:254–264

Enokizono M, Sato N, Morikawa M et al (2017) "Black butterfly" sign on T2*-weighted and susceptibility-weighted imaging: a novel finding of chronic venous congestion of the brain stem and spinal cord associated with dural arteriovenous fistulas. J Neurol Sci 379:64–68

Flanders AE, Settell CM, Friedman DP, Marino RJ, Herbison GJ (1999) The relationship between the functional abilities of patients with cervical spinal cord injury and the severity of damage revealed by MR imaging. AJNR Am J Neuroradiol 20:926–934

Frohman EM, Wingerchuk DM (2010) Clinical practice. Transverse myelitis. N Engl J Med 363(6):564–572

Fugate JE, Lanzino G, Rabinstein AA (2012) Clinical presentation and prognostic facotrs of spinal dural arteriovenous fistulas: an overview. Neurosurg Focus 32(5):E17

Ghandehari K, Gerami Sarabi MR, Maarufi P (2010) Clinical evaluation of patients with spinal cord infarction in Mashad, Iran. Stroke Res Treat 2010:942417

Gross BA, Du R (2014) Spinal juvenile (Type III) extradural-intradural arteriovenous malformations. J Neurosurg Spine 20(4):452–458

Hanson SR, Romi F, Rekand T, Naess H (2015) Long-term outcome after spinal cord infarctions. Acta Neurol Scand 131:253–257

Harringan M, Deveikis J (2013) Handbook of cerebrovascular disease and neurointerventional technique, 2nd edn. Humana Press, New York

Hausmann O, Kirsch E, Radu E et al (2001) Coagulopathy induced spinal intradural extramedullary haematoma: report of thre cases and review of the literature. Acta Neurochir 143:135–140

Jorgensen HS, Nakayama H, Raaschou HO, Olsen TS (1994) Effect of blood pressure and diabetes on stroke in progression. Lancet 344:156–159

Kobayashi K, Imagama S, Ando K et al (2017) Acute non-traumatic idiopathic spinal subdural hematoma: radiographic findings and surgical results with a literature review. Eur Spine J 26:2739–2743

Kreppel D, Antoniadis G, Seeling W (2003) Spinal hematoma: a literature survey with meta-analysis of 613 patients. Neurosurg Rev 26:1–49

Krings T, Mull M, Gilsbach JM et al (2005) Spinal vascular malformations. Eur Radiol 15:267–278

Krings T, Lasjaunias PL, Hans FJ et al (2007) Imaging in spinal vascular disease. Neuroimaging Clin N Am 17(1):57–72

Looby S, Flander A (2011) Spina trauma. Radiol Clin N Am 49(1):129–163

Manara R, Calderone M, Severino MS et al (2010) Spinal cord nfarction due to fibrocartilaginous embolization: the role of diffusion weighted imaging and short-tau inversion recovery sequences. J Child Neurol 25(8):1024–1028

Mascalchi M, Mangiafico S, Marn E (1998) Hematomyelia complicating a spinal dural arteriovenous fistula. Report of a case. J Neuroradiol 25:140–143

Mashiko R, Noguchi S, Uemura K, Takada T, Matsumura A (2006) Lumbosacral subdural hematoma. Neurol Med Chir (Tokyo) 46:258–261

Mateen FJ, Monrad PA, Hunderfund AN, Robertson CE, Sorenson EJ (2011) Clinically suspected fibrocartilaginous embolism : clinical characteristics, treatments, and outcomes. Eur J Neurol 18(2):218–225

Moriarty HK, O'Cearbhail R, Moriarty PD, Stanley ER, Lawler LP, Kavanagh EC (2019) MR imaging of spinal haematoma. Br J Radiol 92(1095):20180532

Naess H, Romi F (2011) Comparing patients with spinal cord infarction and cerebral infarction: clinical characteristics, and short-term outcome. Vasc Health Risk Manag 7:497–502

Naess H, Nyland HI, Thomassen L, Aarseth J, Myhr KM (2005) Fatigue at long-term follow-up in young adults with cerebral infarction. Cerebrovasc Dis 20:245–250

Nedeltchev K, Loher TJ, Stepper F, Arnold M, Schroth G, Mattle HP et al (2004) Long-term outcome of acute spinal ischemia syndrome. Stroke 35:560–565

Novy J, Carruzzo A, Maeder P, Bogousslavsky J (2006) Spinal cord ischemia: clinical and imaging patterns, pathogenesis, and putcomes in 27 patients. Arch Neurol 63(8):1113–1120

Peckham ME, Hutchins TA (2019) Imaging of vascular disorders of the spine. Radiol Clin N Am 57(2):307–318

Pierce JL, Donahue JH, Nacey NC et al (2018) Spinal hematomas: what a radiologist needs to know. Radiographics 38:1516–1535

Pillai A, Crane E, Chappell A et al (2008) Traumatic cervical hematomyelia: report of a rare spinal cord injury without radiographic abnormality. J Trauma 65:938–941

Raghavan A, Onikul E, Ryan MM et al (2004) Anterior spinal cord infarction owing to possible fibrocartilaginous embolism. Pediatr Radiol 28:44–47

Robertson CE, Brown RD, Wijdicks EF, Rabinstein AA (2012) Recovery after spinal cord infarcts: long-term outcome in 115 patients. Neurology 78:114–121

Rodesch G, Hurth M, Alvarez H et al (2004) Angio-architecture of spinal cord aretriovenous shunts at presentation. Clinical correlations in adults in children. The Bicentre experience on 155 consecutive patients seen between 1981-1999. Acta Neurochir 146(3):217–226

Romi F, Naess H (2011) Characteristics of spinal cord stroke in clinical neurology. Eur Neurol 66:305–309

Romi F, Naess H (2016) Spinal cord infarction in clinical neurology: a review of characteristics and long-term prognosis in comparison to cerebral infarction. Eur Neurol 76:95–98

Rosenblum B, Oldfield EH, Doppman JL et al (1987) Spinal arteriovenous malformations: a comparison of dural arteriovenous fistulas and intradural AVMs in 81 patients. J Neurosurg 67:795–802

Rubin MN, Rabinstein AA (2013) Vascular diseases of the spinal cord. Neurol Clin 31(1):153–181

Shaban A, Moritani T, Al Kasab S, Sheharyar A, Limaye KS, Adams HP (2018) Spinal cord hemorrhage. J Stroke Cerebrovasc Dis 27(6):1435–1446

Spengos K, Tsivgoulis G, Toulas P et al (2006) Spinal cord stroke in a baller dancer. J Neurol Sci 15:159–161

Sullivan TM, Sundt TM (2006) Complications of thoracic aortic endograft: spinal cord ischemia and stroke. J Vasc Surg 43(Suppl A):85A–88A

Swann KW, Ropper EH, New PF et al (1984) Spontaneous spinal subarachnoid hemorrhage and subdural hematoma. Report of two cases. J Neurosurg 61:975–980

Vargas MI, Gariani J, Sztajzel R, Barnaure-Nachbar I, Delattre BM, Lovblad KO, Dietermann JL (2015) Spinal cord ischemia: practical imaging tips, pearls and pitfalls. AJNR Am J Neuroradiol 36:825–830

Vuia O, Alexianu M (1969) Arteriovenous shunt in the spinal cord circulation. Acta Neurol Scand 45(2):216–223

Vuong MD, Jeong WJ, Morales H, Abruzzo TA (2016) Vascular diseases of the spinal cord: infarction, hemorrhage and venous congestive myelopathy. Semin Ultrasound CT MR 37(5):466–481

Yousef OM, Appenzeller P, Kornfeld M (1998) Fibrocartilaginous embolism: an unusual case of spinal cord infarction. Am J Forensic Med Pathol 19(4):395–399

Zalewski NL, Flanagan EP, Keegan BM (2018) Evaluation of idiopathic transverse myelitis revealing specific myelopathy diagnoses. Neurology 90(2):e96–e102

Zalewski NL, Rabinstein AA, Krecke KN, Brown RD, Wijdicks EFM, Weinshenker BG et al (2019) Characteristics of spontaneous spinal cord infarction and proposed diagnostic criteria. JAMA Neurol 76(1):56–63